

OBJECTIVE ULTRASONIC CHARACTERIZATION OF WELDING DEFECTS USING
PHYSICALLY BASED PATTERN RECOGNITION TECHNIQUES

S. F. Burch

Materials Physics and Metallurgy Division
Harwell Laboratory
Oxfordshire, UK

INTRODUCTION

Computer-based methods for analysing ultrasonic data to distinguish between different defect types have been based on a variety of techniques such as adaptive learning [1], artificial intelligence [2] and statistical pattern recognition [3]. The uncertain classification reliability of these techniques when applied to a range of realistic defect types has, however, often been a significant practical limitation to their use.

To develop reliable and objective techniques for distinguishing between significant crack-like welding defects and volumetric flaws, the approach adopted at Harwell was first to ensure that sufficient ultrasonic data was available for each reflector. Thus each defect was (raster) scanned in two-dimensions using multiple angles of pulse-echo ultrasound [4],[5], instead of basing the entire classification analysis on single or small numbers of waveforms. Well-understood numerical descriptors (features), each having a clearly defined physical basis, were then computed from these data, to avoid any problems connected with empirically determined features of questionable significance. In [4] the crack-like defects were principally oriented parallel to the inspection surface (horizontal defects) and the characterization techniques were based on the use of pulse-echo transducers giving compression waves with angles of 0, 10 and 20°. In [5] the crack-like defects were lack of sidewall fusion in single V butt welds and characterization was based on multiple angles of shear waves reflected off the backwall, one of which gave normal incidence on the weld fusion face.

This paper describes the extension of the techniques described in [4] and [5] to vertical and near vertical planar defects by use of a combination of 45° pulse-echo and tandem inspection techniques. The aim of the subsequent data analysis was to achieve, as far as possible, compatibility between the feature values derived from these three inspection techniques. This enabled a common database to be built up, containing the results from all the defect scans.

EXPERIMENTS AND DATA RECORDING

Full details of the experimental procedures and data recording techniques used for the two pulse-echo inspection techniques have been given previously [4],[5]. The different ultrasound angles (both compression and shear waves) were obtained by using an immersion probe with variable tilt. For each ultrasound angle, the whole of each defect was scanned in two-dimensions using a stepper-motor driven x-y scanning frame, controlled by a computer-based Zipscan system [6], which was also used for digital recording of complete unrectified RF waveforms at each transducer position.

For the 45° pulse-echo/tandem inspection of the vertical and near-vertical defects similar scanning and recording hardware was used, but the transducers were standard contact 45° shear wave probes (2 MHz, 20 mm diameter). As before, appropriate calibration scans were recorded before and after scanning each defect.

Fig. 1 illustrates the three inspection techniques on which the defect characterization techniques are now based.

DEFECT TYPES

The different types of buried defects examined using each of the three inspection techniques are listed in Table 1. Most of the total of 80 defects were deliberately introduced into welds, although 6 were naturally occurring defects. The minimum dimension of the crack-like defects varied from approximately 5 to 30 mm and all the flaws were intended to be representative of those having possible structural significance in thick and medium sectioned welds (i.e. about 25 to 250 mm wall thickness).

For classification purposes, the first seven defect types in Table 1 were all considered to be crack-like defects, listed in increasing order of surface roughness.

The five "ribbon" defects inspected using the tandem/pulse-echo technique were machined flaws introduced using diffusion welding, with through-wall sizes of 10 and 25 mm and tilts to the vertical of 0 and 7°.

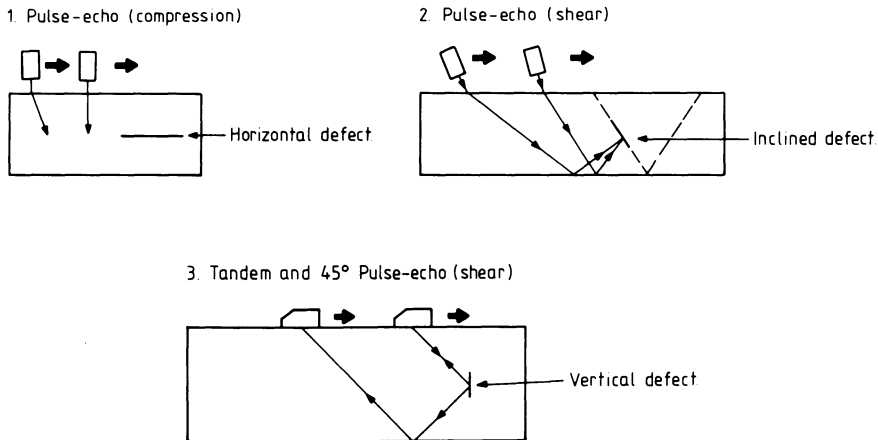


Fig. 1. Schematic illustration of inspection techniques.

Table 1. Defect types

Defect type	No.	Inspection technique		
		Compression	Shear	Tandem/Pulse echo
Lack of fusion	10	*	*	
Unfused land	2	*		
Ribbon defects	5			*
Hydrogen crack	7	*		
Fatigue crack	8	*		
Lamellar tear	3	*		
Carbon crack	17	*		
Inclusions	18	*	*	
Porosity	10	*	*	

TANDEM/PULSE-ECHO IMAGING

The processing and display of the digitised ultrasonic data was carried out using a VAX 11/750 computer linked to an International Imaging Systems display device. Although complete RF waveforms were recorded, the subsequent imaging and feature computation methods were based on envelope detected waveforms, derived from the RF data by the analytic signal method [7].

The three-dimensional imaging techniques developed for the results of two-dimensional (raster) scanning of pulse-echo transducers have been described previously [4],[5]. For the present work, the imaging techniques were extended to the results from the Tandem scans, using the following method.

To calculate a unique (x,y,z) co-ordinate (in the specimen) for each signal arrival time within the Tandem waveforms, it was assumed that the signal was positioned on the centre-line of the ultrasound beam from the nearer transducer. The (x,y,z) co-ordinates of the signal were then calculated from the signal arrival time, the transducer separation, the plate thickness, the (x,y) transducer position, and the velocity and angle of the ultrasound. This enabled positionally corrected plan, side and end view images to be computed from the available three-dimensional echo amplitude data.

Grey-scale coded imaging results from the Tandem scans of two vertical defects (one smooth, one slightly rough) are given in Fig. 2a, which shows the strong specular signals obtained from both defects. Fig. 2b gives the corresponding images obtained from scans of the 45° pulse-echo transducer, with a substantially more sensitive amplitude scale. This image reveals the (much weaker) diffracted signals from the upper and lower tips of both defects. The apparently larger through-wall extent of the Tandem images is merely due to beamwidth effects.

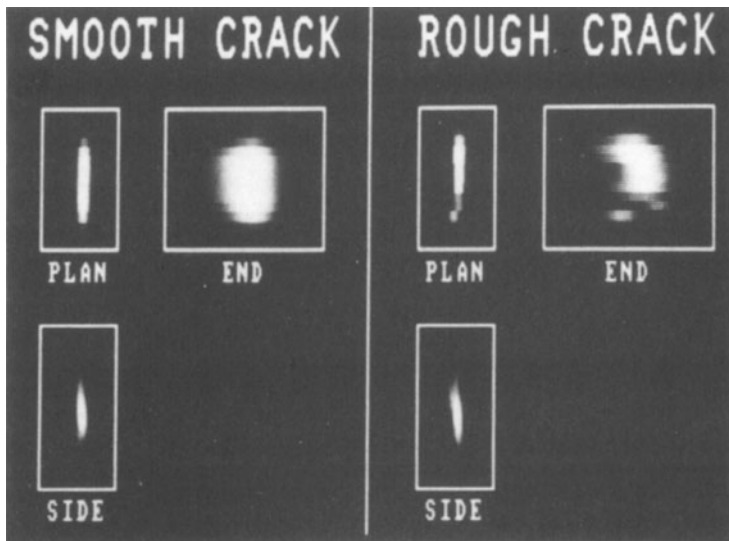


Fig. 2a. Defect imaging results for tandem inspection.

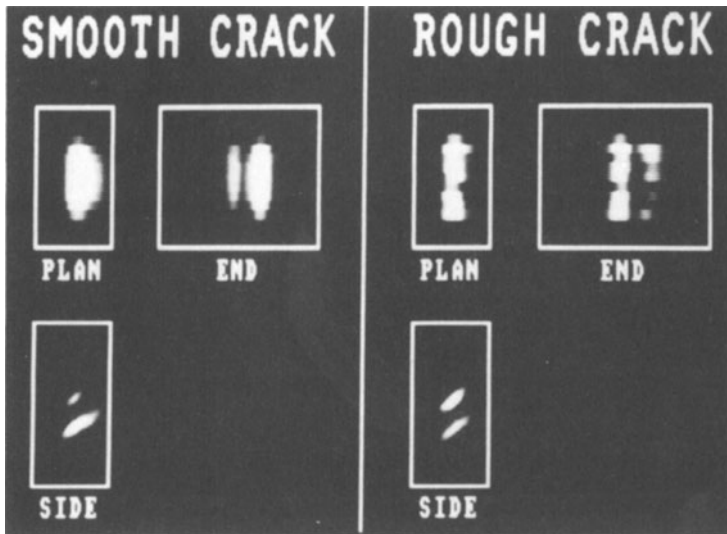


Fig. 2b. Defect imaging results for 45° pulse-echo shear waves.

FEATURE CALCULATION FOR TANDEM/PULSE-ECHO INSPECTION

In the earlier work [4],[5], three features each based on an independent physical effect were selected for objective defect discrimination using results from the compression and shear wave inspection techniques. For the present tandem/pulse-echo inspections, these three features were again calculated and appropriate normalization and calibration methods ensured compatibility with those values previously derived, as follows.

(a) Variation of reflected signal amplitude with ultrasound angle

The feature termed amplitude ratio (AM) was defined as the ratio of the signal amplitudes obtained from the 45° pulse-echo and tandem scans. Normalization of the signal strengths using the calibration scans ensured that spherical reflectors would have an amplitude ratio of approximately one. However, for smooth planar reflectors the AM values so obtained were substantially lower than those previously derived for pulse-echo angles that differed by only 20°. This was expected since the diffracted signals from smooth planar defects for an off-normal angle of 45° are weaker than for 20°. To ensure compatibility with the previously determined AM values of about one for volumetric flaws and about 0.03 for the smoothest planar reflectors, the 45° pulse-echo/tandem AM values were raised to the power of 0.66. (This exponent was determined experimentally from the 45° pulse-echo/tandem AM value obtained from the 25 mm smooth vertical ribbon defect).

(b) Average waveform shape

The average waveform shape from the tandem inspection results was quantified by a statistical parameter known as kurtosis (KU), which provides a measure of the "peakedness" of the waveform [8]. As before, the average waveform kurtosis for each defect response was normalized by that of the calibration waveform to achieve compatible values from different transducers. Single sharply peaked waveforms such as those from smooth crack-like defects or single inclusions gave higher KU values than the multi-peaked waveforms from very rough cracks or porosity.

(c) Apparent 3-D shape of defect

The feature termed sphericity (SP) was used as a measure of the 3-D shape of each defect response on the positionally corrected Tandem data. For a spherically distributed set of recorded signals, the sphericity value would be approximately one, whereas much lower values would be obtained for a planar distribution.

FEATURE VALUES FROM ALL INSPECTION TECHNIQUES

As indicated in Table 1, a total of 80 defects has now been scanned for the defect characterization project, using one of three possible inspection techniques, depending on the orientation of the planar defects.

The compatible feature values obtained from each defect, regardless of inspection technique are shown in the scatter plot given in Fig. 3. The three defect classes (crack-like, inclusions, porosity) are shown by the different symbols. The logarithms of the amplitude ratio and sphericity values were used since this non-linear transformation was found to improve class separation for these two features.

The scatter plot shows that the values for the three defect classes fell into distinct, separate clusters without any overlapping points. There were no obvious differences between the feature values derived from the three inspection techniques. The notably elongated shape of the crack-like defect class was due to variations in surface roughness; as expected, the rough defects gave significantly higher values for AM and lower values for KU than those with smooth surfaces.

CLASSIFICATION BY STATISTICAL PATTERN RECOGNITION

Following [5], the pattern recognition technique known as principal components analysis was used for the classification of the points within the 3-D feature space. This technique gives optimum results only for multivariate normal probability distributions, but was capable of handling any number of clusters of points each with differing shapes and sizes.

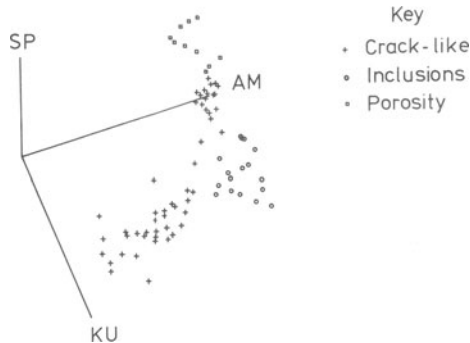


Fig. 3. Scatter plot of feature values for all defects.

To illustrate the separation achieved between defect classes using all 80 defects for "training" the principal components algorithm, Fig. 4 shows a histogram of the values for each defect of the parameter R. This parameter was a normalized measure of the radial distance of each point from the centre of the crack-like defect class, after applying a co-ordinate transformation to make the cluster of the feature values for the crack-like class spherical in shape [5]. For correct classification, crack-like defects should have R values less than one, whereas both classes of volumetric flaws should give R values greater than one. Fig. 4 indeed shows that none of the defects was misclassified, although a few of the volumetric flaws were close to the discrimination value.

A precise statistical assessment of classification reliability is difficult due to the limited numbers of defects currently available in each class, and due to the likelihood that the feature values within each defect class do not have exactly normal probability distributions. An approximate assessment of defect classification performance can, however, be obtained by partitioning the database containing 80 defects in 80 different ways, each time using 79 defects for "training" the principal components algorithm which is then used to classify the remaining one defect. This "leave-one-out" assessment method was applied to the database and a performance index of 97.5 percent was achieved, with two of the porosity flaws being misclassified as crack-like. This is nevertheless a very high performance index compared with that achieved by other approaches. Furthermore, all five of the planar defects scanned with the tandem/pulse-echo technique were correctly classified as crack-like.

CONCLUSIONS

An approach to reliable, objective defect characterization based on 3-D defect imaging using multiple angles of ultrasound, followed by computation of three features, each with a well-defined physical basis had previously been applied to results from 70 buried defects, scanned with two pulse-echo inspection techniques [4],[5]. This approach has been successfully extended to the characterization of planar defects oriented at angles of 0 and 7° to the vertical using a combined 45° pulse-echo/tandem inspection technique.

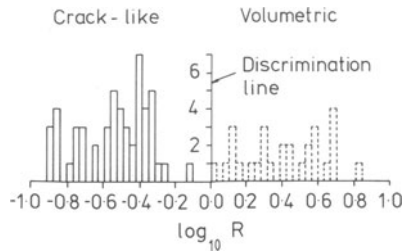


Fig. 4. Separation achieved between crack-like defects and both types of volumetric flaw, using a principal components algorithm for statistical pattern recognition.

The Harwell defect characterization database now has results from 80 defects scanned using any one of three inspection techniques, depending on the orientation of the planar reflectors. Calibration and normalization methods were used to ensure that the three inspection techniques gave mutually compatible feature values.

The feature values for the three defect classes (crack-like, inclusions, porosity) fell into distinct, separate clusters without any overlapping points. An approximate estimate of the reliability of classification using the principal components algorithm for statistical pattern recognition gave a performance index of 97.5 percent, with two volumetric flaws being misclassified as crack-like. This value was based on a "leave-one-out" method in which independent data are used for algorithm training and classification. No classification errors were, however, obtained using the same data for both training and classification.

Although this approach to defect characterization is, in principle, based upon detecting specular reflections from smooth planar defects, the method was shown to be insensitive to a tilt of 7° in defects inspected

using the combined 45° pulse-echo/tandem inspection technique.

ACKNOWLEDGEMENTS

The author is indebted to N. Bealing for carrying out much of the experimental work upon which this paper is based and to Dr. J. C. Collingwood for valuable discussions. The Welding Institute, England is also thanked for the loan of the specimens that contained naturally occurring defects. Some of the work described in this paper was undertaken as part of the Underlying Research Programme of the UKAEA.

REFERENCES

1. M. F. Whalen, L. J. O'Brien, and A. N. Mucciardi, Proceedings of the DARPA/AFML Review of Progress in Quantitative NDE, AFWAL-TR-80-4078, 1980.
2. L. W. Schmerr, K. E. Christensen, and S. M. Nugen, in Review of Progress in Quantitative NDE, edited by D. O. Thompson and D. E. Chimenti (Plenum Press, New York, 1987), Vol. 6A, pp. 879-887.
3. J. L. Rose, J. Nestleroth, L. Niklas, O. Ganglbauer, J. Ausserwoeger, and F. Wallner, *Materials Eval.*, 42, 433-438, 443 (1984).
4. S. F. Burch, and N. K. Bealing, *NDT International*, 19, 145-153 (1986).
5. S. F. Burch, and N. K. Bealing, paper presented at 21st Annual British Conference on NDT, Newcastle, Sept. 1986.
6. B. J. Smith, *Brit. J. NDT*, 28, 9-16 (1986).
7. P. M. Gammell, *Ultrasonics*, 19, 73-76 (1981).
8. G. P. Singh, and R. C. Manning, *NDT International*, 16, 325-329 (1983).